Effect of temperature and dissolved oxygen content on the dissolved iron concentration in liquid sodium at equilibrium

Sami Meddeb, Jean-Louis Courouau, Marion Rouhard, Nelly Cavaliere, Marie-Laurence Giorgi

Version of Record: https://www.sciencedirect.com/science/article/pii/S0022311522002720
Manuscript_63f5e6946549f2dde3b486ffae1d68ad

Effect of temperature and dissolved oxygen content on the dissolved iron concentration in liquid sodium at equilibrium

Sami Meddeb[a,b], Jean-Louis Courouau[a,*], Marion Rouhard[a], Nelly Cavaliere[a], Marie-Laurence Giorgi[b,*]

[a] Université Paris-Saclay, CEA, Service de la Corrosion et du Comportement des Matériaux dans leur Environnement, 91191, Gif-sur-Yvette, France
[b] Université Paris-Saclay, CentraleSupélec, Laboratoire de Génie des Procédés et Matériaux, 91192, Gif-sur-Yvette cedex, France

*Corresponding author

Email address: marie-laurence.giorgi@centralesupelec.fr
jean-louis.courouau@cea.fr

Highlights

- The corrosion mechanism of pure iron by liquid sodium is homogeneous dissolution.
- The dissolution of iron in liquid sodium increases with dissolved oxygen content.
- Dissolved Fe content is measured for dissolved O contents less than 400 ppm at 550 °C
- A soluble complex (Na-Fe-O) is formed in liquid sodium.
- A thermodynamic law is given to estimate the dissolved Fe content in oxygenated Na

Abstract

This study aims to determine the effect of temperature and dissolved oxygen content on the dissolved iron concentration in liquid sodium at equilibrium. Based on the mass variation of the samples, the applied experimental approach avoids the conventional but inaccurate chemical analysis that requires representative samples of liquid metal so that trace amounts of corrosion products can be measured. The results obtained show that, under isothermal conditions at $550\ °C$, the equilibrium iron concentration follows a power law of an order very close to 2 as a function of the initial oxygen content. These results demonstrate unequivocally that the increase in the iron solubility, in the presence of dissolved oxygen, is directly related to a chemical reaction of complexation. The presence in solution of this corrosion product was hypothesized over more than 50 years ago. The stoichiometry of this soluble complex is thought to be $NaFeO_2$. Based on this interpretation and on our experimental measurements, an equilibrium law of this complex in liquid sodium was developed as a function of temperature and dissolved oxygen content. This analytical law can be extrapolated to low dissolved oxygen contents, provided that the contribution of atomic iron to the total dissolved iron in solution is taken into account.

1. Introduction

This work is part of the research carried out by the French Alternative Energies and Atomic Energy Commission (CEA) to maintain the expertise developed on sodium-cooled fast reactors (SFR). These 4th generation nuclear reactors use liquid sodium as a heat transfer fluid due to its low viscosity, low density, good neutron and thermal properties, and compatibility at high temperatures with the structural materials [1]. In addition, under the normal operating conditions of a heat transfer loop, namely a maximum temperature of $550\ °C$ and a dissolved oxygen content of less than $\sim 10\ ppm$, the primary advantage of using liquid sodium over other liquid metals is its minimal corrosion of the structural steel ($316L(N)$ steel). However, although of a low level, this corrosion does exist and consists of a mass loss in the hot leg, which results in a thickness loss, and a deposit in the cold leg. Therefore, this corrosion must be quantified if a reactor lifetime of at least $60\ years$ is to be guaranteed.

Accurate measurements of metal solubility in liquid sodium can improve our understanding of the corrosion process of $316L$ steel by liquid sodium. Indeed, the driving force for dissolution strongly depends on the solubility of the element. One of the crucial parameters is the level of dissolved oxygen in liquid sodium. However, to date, the corrosion mechanisms of metals by liquid sodium in the presence of dissolved oxygen are not fully understood. This is particularly true for iron corrosion despite numerous data available in the literature.

Several research laboratories [1] have taken an active interest in investigating the solubility of iron in liquid sodium, since iron is the major element in structural steels. According to the data in the literature, summarized by Awasthi and Borgstedt [2], data for iron solubility in the presence of dissolved oxygen vary in some cases by three orders of magnitude [3-4]. This large dispersion can be explained by the difficulty of controlling the chemistry of liquid sodium, in particular the dissolved oxygen content, and by the different techniques used, such as radiochemistry and spectrometry. Another significant source of errors arises from sodium sampling [2,5]. Precipitation of iron particles is likely to happen during this sampling operation. In addition, the solubility measurements are usually performed after solidification of the molten sodium, which could cause inhomogeneity of the samples.

Despite these measurement difficulties, it is generally accepted that the iron solubility is an increasing function of the oxygen content in liquid sodium [6]. According to Shaiu's data [7], $Na-Fe-O$ solid oxides require high dissolved oxygen contents in order to form on the iron surface (at least $1000\ ppm$ at $550\ °C$ for Na_4FeO_3). $Na-Fe-O$ ternary oxides are therefore thermodynamically unstable under normal operating conditions and cannot be involved in iron corrosion. Nevertheless, the effect of dissolved oxygen can be explained by assuming that one or more $Na-Fe-O$ complexes, soluble in liquid sodium, will form [8-12]. This assumption will be considered here to establish an analytical law giving the equilibrium concentration of dissolved iron in liquid sodium as a function of oxygen content and temperature. To our knowledge, such a law does not exist in the literature.

To this end, the main objectives of this work are:

1. To obtain accurate experimental measurements of the equilibrium iron concentration in liquid sodium at different temperatures and dissolved oxygen contents (at $550\ °C$ and $50, 100, 200$ and $400\ ppm$; at $600\ °C$ and $200\ ppm$).

[1] e.g. U.S. Naval Research Laboratory (NRL), UK Atomic Energy Authority (UKAEA), Brookhaven National Laboratory (BNL), Atomics International (AI), Knolls Atomic Power Laboratory (KAPL) and Mine Safety Appliances (MSA)

2. To develop an analytical law, allowing the equilibrium iron concentration in liquid sodium as a function of both temperature and dissolved oxygen content to be determined using thermodynamics considerations.

3. To compare the new law obtained with data from the literature.

2. Materials, device, experimental conditions and characterization method

2.1 Pure iron and sodium

In the experiments reported here, iron strips taken from a $0.12\ mm$ thick sheet with $99.95\ wt.\%$ purity, supplied by Neyco, were used to perform the corrosion tests. The size of the iron strips was $40 \times 30 \times 0.12\ mm^3$ or $45 \times 35 \times 0.12\ mm^3$, depending on the corrosion test. No mechanical polishing was performed, and the average roughness was estimated to be $Ra = 96\ nm$, using a Bruker Contour GT interferometer. Previous experiments have shown that the surface roughness of $316L$ steels does not affect the corrosion results [13]. Similarly, the iron dissolution in the experiments reported here showed no significant difference between the as-received strips and the polished ones (up to $1\ \mu m$ diamond suspension). The average chemical composition of the iron strips is given in Table. 1.

	Fe	C	Mn	Cu	Si	Cr	Mo	Ni
(wt.%)	$Balanced$	0.002	< 0.005	< 0.015	0.005	< 0.006	0.005	0.004

Table. 1. Nominal chemical composition of the iron strips (wt.%)

Several preparation steps are necessary before immersing the samples in liquid sodium. First, a $1\ mm$ diameter hole was drilled in the samples so they could be suspended from the sample holder by a molybdenum wire. Numbers were engraved into the samples to identify them. Then, their dimensions were measured precisely with a micrometric caliper. After ultrasonic degreasing in a pure ethanol bath for $10\ min$, the samples were weighed using a Mettler Toledo balance, with an uncertainty of $\sim 20\ \mu g$ for samples of about $5\ g$.

The sodium used in this work was supplied by Métaux Spéciaux S.A and has a high purity of $99.95\ wt.\%$. According to the supplier, the principal impurities are calcium $< 2\ ppm$, chlorine $\sim 4\ ppm$, iron $\sim 1\ ppm$ and potassium$\sim 4\ ppm$. Surface oxides were removed from the sodium ingots by peeling in a glove box under an argon atmosphere before melting.

2.2 Experimental conditions

The corrosion tests were performed in the CORRONa device [13-16], a static sodium testbed operating in a purified argon atmosphere (less than $5\ vpm$ of oxygen and $10\ vpm$ of water vapor). The liquid sodium is contained in a molybdenum crucible, with an internal diameter of $147\ mm$ and height of $250\ mm$, and placed in a resistance-heated furnace. The choice of molybdenum as the crucible structural material is based on Kolster's work [17], which showed that dissolution of molybdenum in sodium is negligible in a circuit made of molybdenum [13]. Accessing the liquid sodium pot through the glove box allows the preparation and end-of-test operations to be carried out at temperatures between 110 and $120\ °C$.

The sodium is melted at $\sim 150\ °C$. Due to surface tension effects, sodium oxides float on the free surface of the liquid sodium and are removed by skimming operations, initially at $150\ °C$. The liquid sodium is maintained at a low temperature ($110\ °C$) for at least $60\ h$ to trigger

crystallization of sodium oxides on the free surface. The floating oxides formed are removed by skimming. The liquid sodium level is adjusted by removing excess sodium. The final mass of sodium in the crucible is estimated to be $2.3 \pm 0.1\,kg$ or $100 \pm 4\,mol$. High-temperature purification ($650\,°C$ for $70\,h$) is then carried out by immersing a zirconium sheet ($200x200x0.1\,m^3$) in the liquid sodium bath. It should be noted that the solubility of zirconium in sodium is negligible, $\sim 0.09\,ppm$ at $650\,°C$ [1]. Preliminary tests validated the purification step at $650\,°C$ since zirconium did not gain mass during an additional identical operation. The zirconium foil is then removed after the liquid sodium bath is cooled to $120\,°C$. The purification method significantly reduces residual oxide and dissolved oxygen in liquid sodium through the formation of zirconium oxides [13]. It is estimated that the sodium contains less than $1\,ppm$ of oxygen after the purification step. For each corrosion test, the sodium is renewed to avoid the accumulation of corrosion products.

Controlled oxygen content is then added to achieve the chemical conditions of the test under consideration ($50, 100, 200$ or $400\,ppm$). A so-called solid pollution technique was applied and consisted of adding a given mass of sodium peroxide (Na_2O_2), supplied by Métaux Spéciaux S.A, into liquid sodium. This step assumes a total dissolution reaction of Na_2O_2 in liquid sodium.

The last step is to immerse the samples, attached to the sample holder, in the liquid sodium bath at $120\,°C$ and close the system tightly. Then the pot is pressurized to $0.3\,bar$, and the temperature rise begins with a gradient of $2\,°C/min$. The corrosion time is counted when the temperature reaches 97% of the target test temperature.

The sodium is evacuated using a ladle at the end of each test, and disposed of via the Saclay center's disposal channel. The molybdenum crucible and all internal components are scraped in a glove box to remove as much residual sodium as possible, then washed with water in the laboratory's dedicated fume cupboard. After thorough rinsing with water, meticulous cleaning and autoclaving, all these components are ready to be used for a new test.

2.3 Performed tests

Five corrosion tests were conducted to determine the effect of temperature and dissolved oxygen content on the dissolved iron concentration in liquid sodium at equilibrium, $w_{Fe}^{Na,eq}$. This quantity is expressed in milligrams of dissolved iron per kilogram of sodium ($mg.kg^{-1}$, parts per million, ppm).

All corrosion tests were performed under static conditions using the interrupted tests principle (Fig. 1). The samples are removed one by one after a selected corrosion time. The liquid sodium is cooled to 120°C and reheated to the test temperature to facilitate sample removal. The average transient thermal cycle time is estimated to be $\sim 20\,h$. The corrosion parameters, time and temperature, are estimated when the sodium temperature exceeds 97% of the test temperature. The test temperature reported is the average temperature of the entire cycle in this temperature range (e.g. $550 +/- 2\,°C$, Fig 1). The corrosion time reported for each sample does not consider transient regimes. The interrupted test method allows the evolution of the mass loss of samples as a function of their immersion time in liquid sodium to be determined, if it is assumed that all the samples behave identically and the corrosion products are stable at low temperatures. This last assumption will be discussed in section 4.1.

For each test, nine samples were initially immersed in liquid sodium. The reaction surface area of the sample was estimated using Eq. 1:

$$S_{r,sample} = 2.[(l.w) + (l.e) + (w.e) - (\pi.r^2)] + (2.\pi.r)e \quad (1)$$

with $S_{r,sample}$: the reaction surface of the sample (m^2), l: the sample length (m), w: the sample width (m), e: the sample thickness (m), and r: the radius of the drilled hole, $r = 1\ mm$. Factor 2 considers the contribution of both sides of the sample in the corrosion process.

The same approach was applied for all tests to estimate $w_{Fe}^{Na,eq}$. A chemical equilibrium was assumed to be achieved in the solution when a similar mass change was obtained for several samples removed from liquid sodium at different immersion times. If no chemical equilibrium was achieved after removal of the nine initially immersed samples, additional samples were immersed. Once iron dissolution stopped, $w_{Fe}^{Na,eq}$ was evaluated by considering the mass loss of all samples immersed in the liquid sodium. The value of $w_{Fe}^{Na,eq}$ is the total mass of dissolved iron divided by the total mass of liquid sodium ($2.3 \pm 0.1\ kg$).

The conditions for conducting the corrosion tests (total time, t, average temperature, T, dissolved oxygen content, w_O^{Na}, initial reaction surface, $S_{initial,r}$, and the number of samples added during the test, $N_{during,t}$), are given in Table 2. For clarity, a numerical designation including the temperature and dissolved oxygen content was used to specify the tests. For example, a test performed at $550\ °C$ and $100\ ppm$ of dissolved oxygen is denoted T550-100.

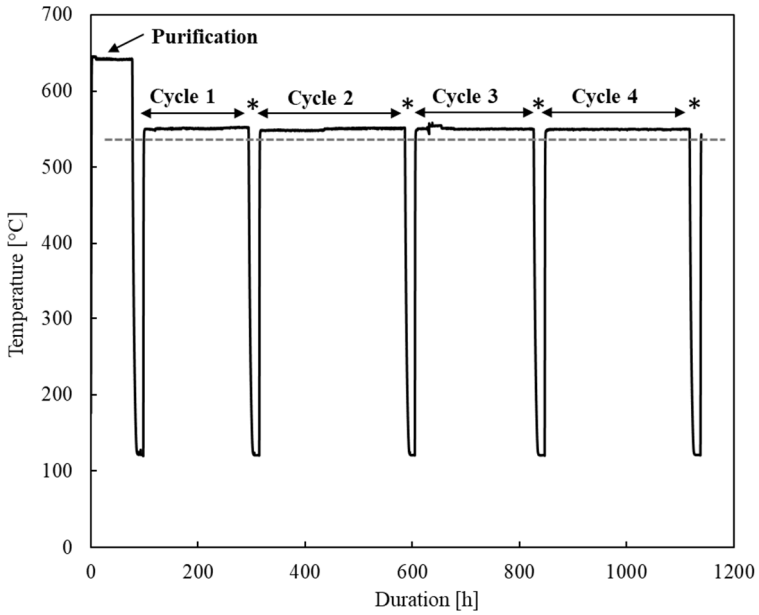

*Fig. 1. Thermal cycle of a corrosion test performed at 550 °C. Reductions in the temperature to 120 °C allow the samples to be removed from the liquid sodium for analysis. *: corresponds to a sample removal. The gray dashed line corresponds to* 97% *of the target test temperature.*

	$t\ (h)$ [a]	$T\ (°C)$ [b]	$w_O^{Na,init}\ (ppm)$ [c]	$S_{initial,r}\ (dm^2)$ [d]	$N_{during,t}$ [e]
T550-50	2410	552 ± 2	50 ± 2	2.15 ± 0.05	0
T550-100	4365	550 ± 2	100 ± 4	2.17 ± 0.05	24
T550-200	4796	550 ± 2	200 ± 8	2.86 ± 0.05	27
T550-400	4078	550 ± 2	400 ± 16	2.18 ± 0.05	21
T600-200	7560	602 ± 2	200 ± 8	2.17 ± 0.05	38

Table 2. Operating conditions of the five performed tests.[a] corrosion time; [b] bath temperature; [c] dissolved oxygen content in liquid Na; [d] reaction surface area of the nine initially immersed samples; [e] number of additional samples added during the test.

2.4 Characterization techniques

Once removed from the liquid sodium, the samples were ultrasonically degreased in a pure ethanol bath for $10\ min$ to remove metallic sodium residues.

A Mettler Toledo scale, model XP205, was used to weigh the samples before and after the corrosion tests. The roughness of the samples was measured using a Bruker Contour GT interferometer. Scanning Electron Microscopy (SEM, ZEISS FEG GEMINI ULTRA 55 Model) was used to perform surface and polished cross-section characterization of the samples. Energy dispersive X-ray spectroscopy (EDX, AXS Flash 4010 Bruker Detector) was also carried out to determine the average composition of the analyzed surface. The cross-sections were prepared using a hot embedding process.

3. Corrosion test results

3.1 Characterization of the sample surfaces after a complete corrosion test

After exposure to liquid sodium, the surfaces of the samples were systematically characterized by SEM. Fig. 2 shows the results obtained for a sample exposed to liquid sodium at $550\ °C$ and $200\ ppm$ of dissolved oxygen for $1195\ h$. These results are representative of all our samples.

As shown in Fig. 2.a, except for a few white spots of sodium residue, the surface of the samples is free of corrosion products. Thus, no solid ternary oxides of iron and sodium, which are insoluble in ethanol [3], are formed on the samples under our operating conditions. Our SEM observations are in good agreement with thermodynamic calculations of the stability of $M-Na-O$ ternary oxides [7,13].

The surface morphology is consistent with iron dissolution and shows slightly faster dissolution at the grain boundaries than at the grain surface. Fig. 2.a also shows the formation of streaks at the grain surface. This phenomenon is related to the surface dissolution, which depends on the crystal orientation of the grains. In general, these streaks become sharper with increased duration of exposure to liquid sodium and with higher temperatures [18]. The sample cross-section, given in Fig. 2.b, shows a homogeneous interface.

Additional EDX analysis (Fig. 3) also showed a uniform and homogeneous corrosion interface, with no apparent variation in chemical composition. A thin layer of sodium residue remains on the sample surface, even after ultrasonic degreasing with pure ethanol. Nevertheless, this is not an oxide layer since it does not contain iron. The presence of oxygen on the surface indicates that this layer is probably sodium hydroxide, $NaOH$, which results from the reaction of sodium ethanolate C_2H_5ONa with moist air.

All these observations confirm that the mechanism of corrosion of pure iron by liquid sodium corresponds to homogeneous dissolution. The average iron dissolution rate, $R_{C,i}\ (mg/dm^2/h)$, after a period of time $\Delta t_i\ (h)$, can thus be estimated using Eq. 2:

$$R_{C,i} = \frac{\Delta m_i}{S_{r_i} \cdot \Delta t_i} \tag{2}$$

with Δm_i: the sample mass variation (mg) and S_{r_i}: the sample reaction surface (dm^2).

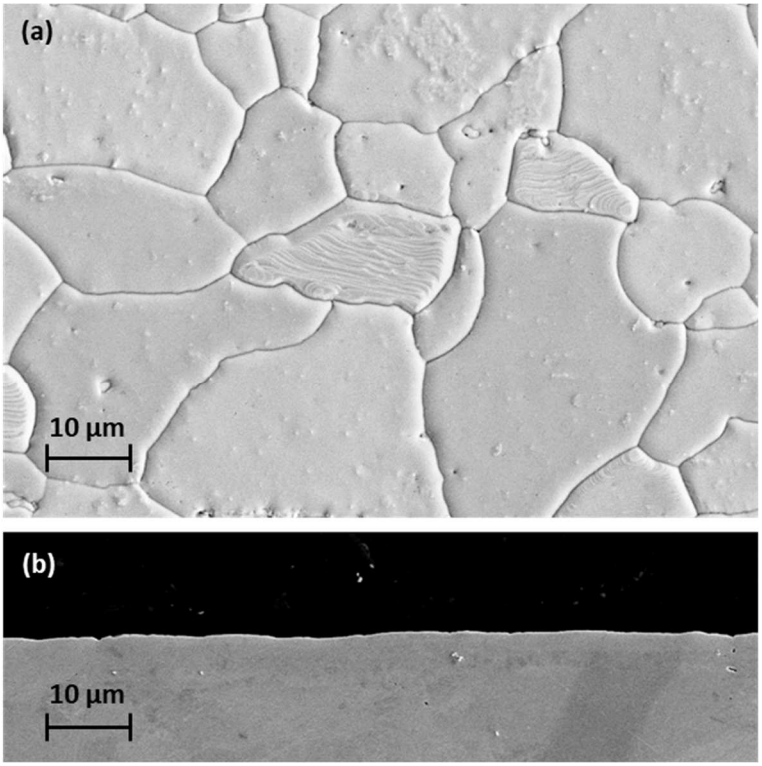

Fig. 2. SEM observation of a sample immersed in liquid sodium for 1195 h at 550 °C and 200 ppm of dissolved oxygen. (a): surface and (b): cross-section. The mounting resin appears in black, and iron appears in grey. No solid oxide is visible on the sample surface.

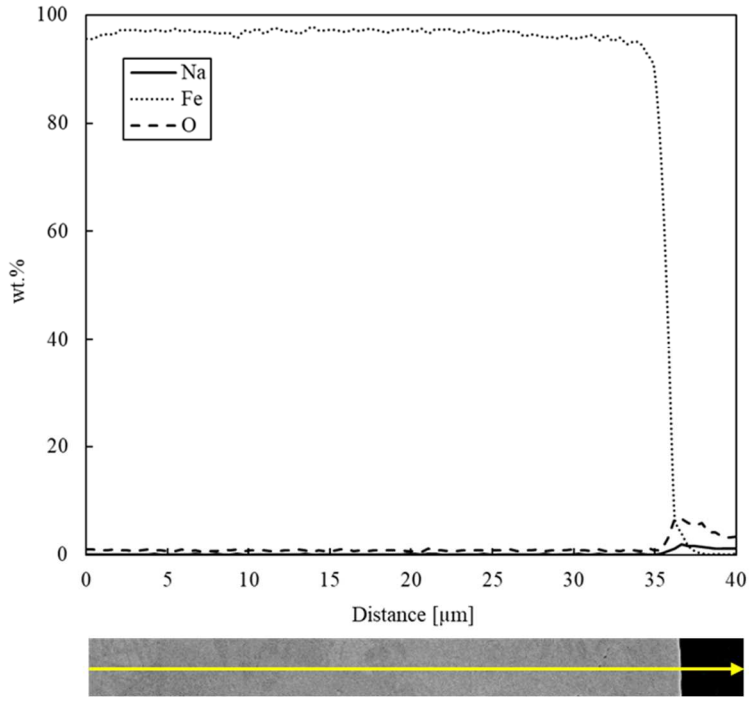

Fig. 3. EDX elemental concentration profile across the corrosion interface of a sample (yellow arrow on the bottom cross-section) after immersion in liquid sodium for 1195 h at 550 °C and 200 ppm of dissolved oxygen. The surface is mainly composed of iron despite residues from washing that remain on the surface (probably NaOH).

3.2 Effect of dissolved oxygen on the dissolved iron concentration in liquid sodium at equilibrium at 550 °C

The effect of dissolved oxygen on the dissolved iron concentration in liquid sodium at equilibrium, $w_{Fe}^{Na,eq}$ (ppm), was studied with 4 tests at different oxygen contents ($50, 100, 200$ and $400\ ppm$) and an average temperature of $\sim 550 \pm 2\ °C$ (Table 2).

For each experimental condition, the sample mass loss was plotted as a function of immersion time in liquid sodium (Fig. 4). The solid symbols represent the behavior of the nine initially immersed samples. Thermodynamic equilibrium between pure iron and oxygenated sodium was not reached at this step. New samples were then immersed in liquid sodium. The hollow symbols correspond to these samples.

For the T550-400 test (Fig. 4.a), the evolution of the mass loss of the samples as a function of immersion time in liquid sodium is linear up to $2083\ h$ for the first nine samples. The test was continued by adding nine new samples to liquid sodium. Dissolution continues until the obvious change in the slope of the dissolution line. The mass loss of the last five samples is almost constant. It can be assumed that a chemical equilibrium was reached at that point between pure iron and the liquid sodium bath. In order to confirm this, three more samples were added to the liquid sodium. The mass of these three samples remains constant after 149 and $200\ h$ of immersion. This result confirms that the approach used is valid for determining $w_{Fe}^{Na,eq}$. The $w_{Fe}^{Na,eq}$ value was then estimated to be $39 \pm 2\ ppm$ from the mass losses of all samples. It should be noted that one of the 9 samples immersed in liquid sodium during the test got detached and was then removed at the end of the test. The mass loss of this sample, evaluated at $9.8 \pm 0.2\ mg/dm^2$, was not included in Fig. 4.a.

Similar evolutions were observed for the mass variation of the samples for tests T550-200 (Fig. 4.b) and T550-100 (Fig. 4.c). In both cases, several additional samples were required to obtain a change in the slope of the dissolution line ($4487\ h$, Fig 4b and $3776\ h$, Fig 4c). It should be noted that a large iron sheet, with a reactive surface area of $8.4 \pm 0.1\ dm^2$, was immersed in liquid sodium during both tests, after $4422\ h$ and $3381\ h$, respectively. The idea was to increase the total reactive surface area to reach chemical equilibrium faster. An accurate measurement of the mass variation of the iron sheet was not possible. In order to overcome this issue, the following assumption was made: the mass loss of the iron sheet was assumed to be the same per unit area as for the samples added at the same time. The $w_{Fe}^{Na,eq}$ values are estimated to be $14.5 \pm 0.8\ ppm$ for liquid sodium containing $200\ ppm$ of oxygen, and $4.7 \pm 0.6\ ppm$ for liquid sodium containing $100\ ppm$ of oxygen.

Regarding the T550-50 test (Fig. 4.d), the change in sample mass was within the measurement uncertainty ($< 1\ mg/dm^2$). The change in the dissolution line slope was observed for the last five samples removed from the liquid sodium. However, we measured a mass gain for these samples. This mass gain is probably explained by the end of iron dissolution due to chemical equilibrium, combined with a slight penetration of sodium into the grain boundaries, which could not be removed by ultrasonic cleaning. To estimate the effective mass loss at the end of this test, we assumed that the last five samples had lost the same mass as the fourth sample removed before chemical equilibrium was established, i.e. $-0.8 \pm 0.1\ mg/dm^2$. With this assumption, the $w_{Fe}^{Na,eq}$ value was estimated to be $0.6 \pm 0.2\ ppm$.

In this paper, we are mainly interested in describing the equilibrium between pure iron and the liquid sodium bath containing dissolved oxygen. The dissolution kinetics of iron, which result in a

linear evolution of the mass loss as a function of time, can be evaluated using Eq. 2. The interpretation of the effect of oxygen on the dissolution kinetics will be the subject of a future publication.

In agreement with Ref. [6], the experimental data of $w_{Fe}^{Na,eq}$ (ppm) obtained at $550\ °C$ increase as the initial dissolved oxygen content, $w_O^{Na,init}$ increases (Fig. 5). $w_{Fe}^{Na,eq}$ follows a power law with an order very close to 2, as a function of $w_O^{Na,init}$. By exploiting these experimental data, an equilibrium law for dissolved iron in liquid sodium can be developed as a function of dissolved oxygen content. This analysis will be the subject of section 4.3.

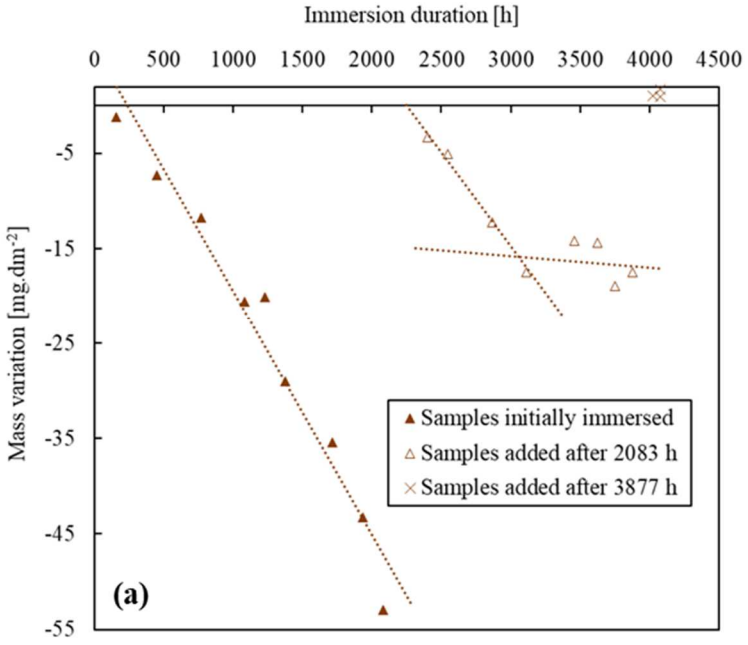

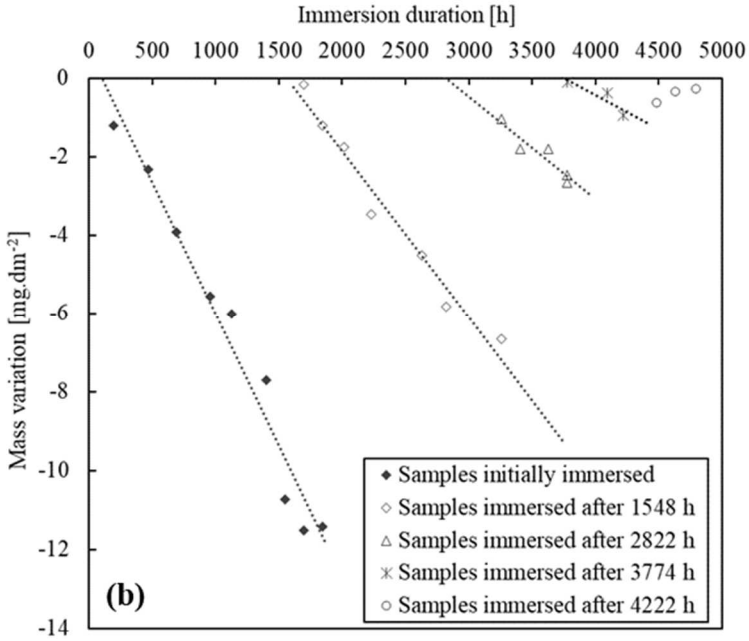

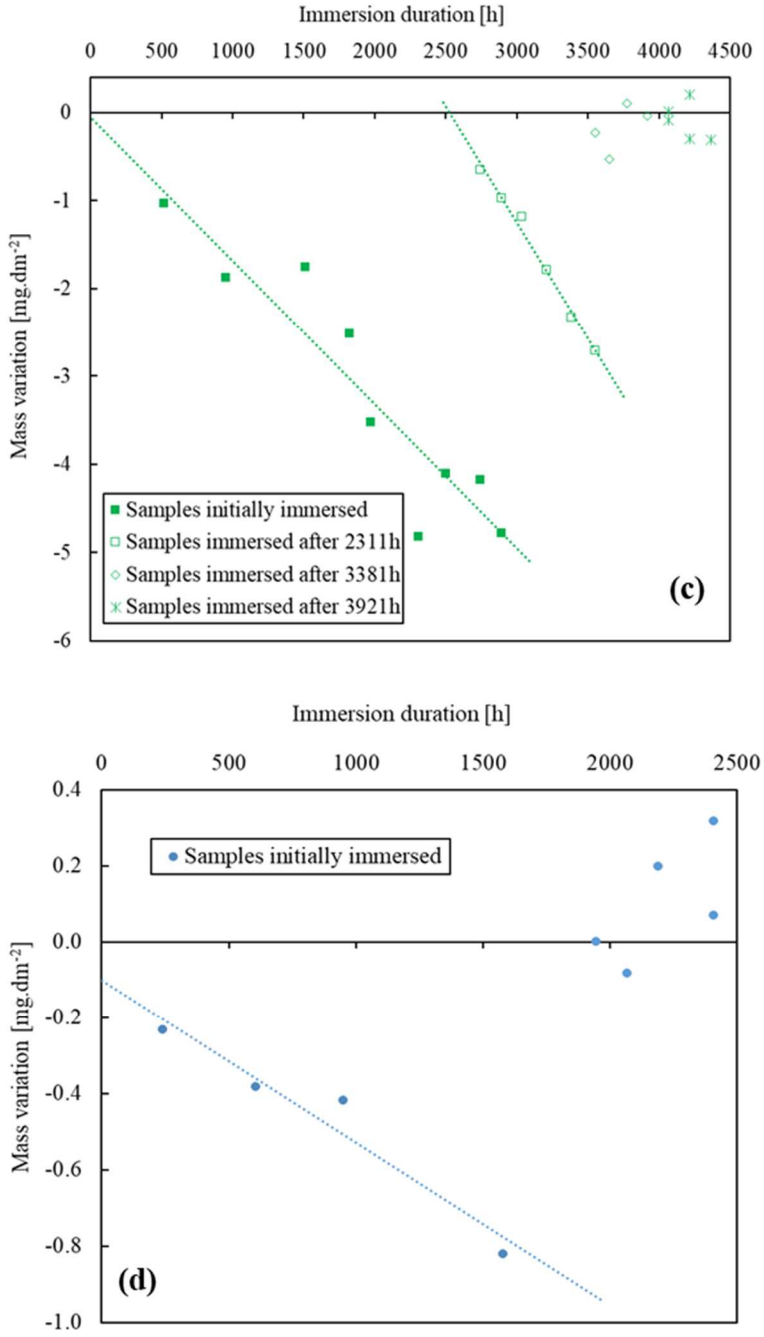

Fig. 4. Establishment of chemical equilibrium between pure iron and a liquid sodium bath containing dissolved oxygen for the tests performed at 550 °C. (a): 400 ppm O, test T550-400, (b): 200 ppm O, test T550-200, (c):100 ppm O, test T550-100 and (d): 50 ppm O test T550-50. Solid symbols: samples immersed initially; hollow symbols: samples added during the test.

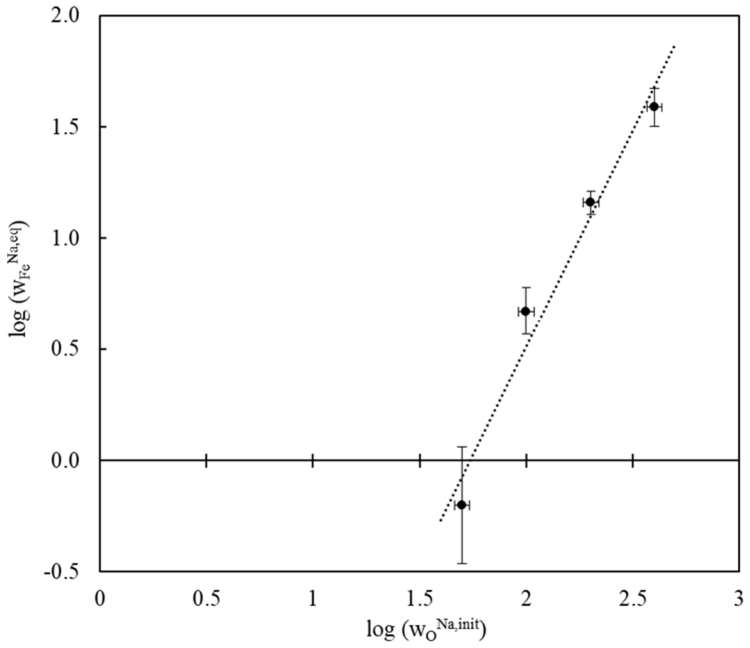

Fig. 5. A log-log plot of the variation in the mass fraction of iron in liquid sodium at equilibrium as a function of the initial dissolved oxygen content at 550 °C. The power function shows a dependence coefficient of 2.

3.3 Effect of temperature on the dissolved iron concentration in liquid sodium at equilibrium

The effect of temperature on the dissolved iron concentration in liquid sodium at equilibrium was studied by performing an additional test at 600°C (T600-200, Table 2). The mass decrease of the samples is plotted as a function of immersion time in Fig. 6. In the same way as for 550°C, after five additional samples and immersion of a large iron sheet of $8.4 \pm 0.1\ dm^2$ after $6653\ h$, the dissolution of iron stops ($\sim 6826\ h$). The $w_{Fe}^{Na,eq}$ value was then evaluated to be $85 \pm 5\ ppm$. The temperature increase of $50\ °C$ leads to an increase in $w_{Fe}^{Na,eq}$ by a factor of ~ 6 ($14.5 \pm 0.8\ ppm$ at $550\ °C$ for the T550-200 test) for the same oxygen content in liquid sodium.

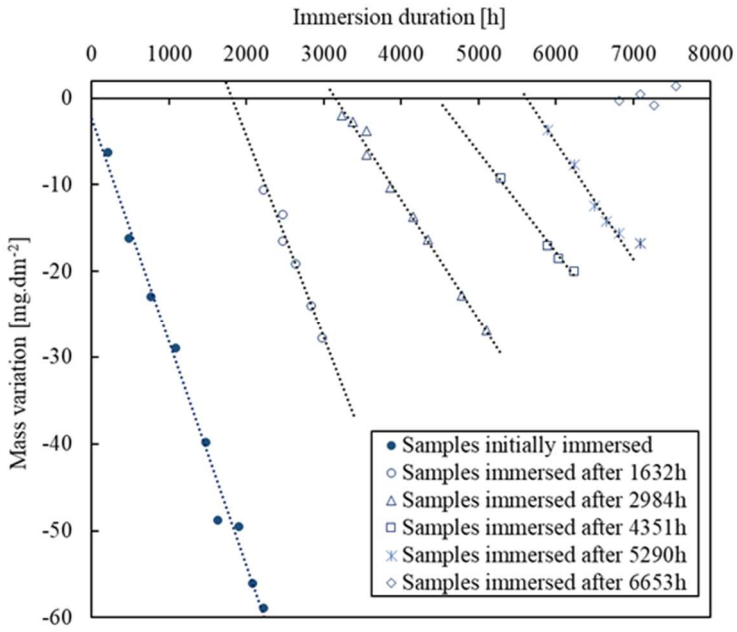

Fig. 6. Establishment of chemical equilibrium between pure iron and a liquid sodium bath containing 200 ppm O at 600°C (test T600-200). Solid symbols: samples immersed initially; hollow symbols: samples added during the test.

4. Discussion

4.1 The form of dissolved iron in liquid sodium

The measurements of dissolved iron concentration in the liquid sodium obtained at different temperatures and different dissolved oxygen contents are summarized in Table 3.

	T550-50	T550-100	T550-200	T550-400	T600-200
$T\ (°C)$	552 ± 2	550 ± 2	550 ± 2	550 ± 2	602 ± 2
$w_O^{Na,init}\ (ppm)$	50 ± 2	100 ± 4	200 ± 8	400 ± 16	200 ± 8
$w_{Fe}^{Na,eq}\ (ppm)$	0.6 ± 0.2	4.7 ± 0.6	14.5 ± 0.8	39 ± 2	85 ± 5

Table 3. Dissolved iron concentration at equilibrium obtained experimentally at different temperatures and dissolved oxygen contents.

The question now is what form the dissolved iron takes.

Let us first consider the atomic iron in liquid sodium. At the U.S. Naval Research Laboratory (NRL), Baus, Bogard et al. [20] conducted one of the most cited works in the literature on the solubility of atomic iron in liquid sodium s_{Fe}^{Na}, i.e., the concentration of atomic iron in liquid sodium in equilibrium with solid iron. They immersed radioactive iron strips in liquid sodium containing low dissolved oxygen content ($w_O^{Na} < 30\ ppm$). The purified liquid sodium was contained in a 347 stainless steel crucible. A radiochemical counting technique was then used to determine s_{Fe}^{Na}. Using the experimental data, the authors developed a solubility law, valid for a temperature $230 < T\ (°C) < 544$:

$$s_{Fe}^{Na} = 2.28 \cdot 10^{-3} - 1.63 \cdot 10^{-5} \cdot T + 5.63 \cdot 10^{-8} \cdot T^2\ (ppm) \quad (3)$$

with T the temperature ($°C$). Extrapolating the law to the temperatures in our study, Eq. 3 estimates a solubility value of $0.010\ ppm$ at $550\ °C$ and $0.012\ ppm$ at $600\ °C$. Later, Singer et al. [21] mentioned in their work that measurement of s_{Fe}^{Na}, at 650 and $750\ °C$, was made by Fleitmann and Isaacs [2] in the Brookhaven National Laboratory (BNL). The liquid sodium, purified using a uranium getter, was contained in a molybdenum crucible. Polley and Skyrme [22] developed a solubility law from these experimental data:

$$s_{Fe}^{Na} = 10^{-0.89-\frac{2347}{T}}\ (ppm) \tag{4}$$

with T the temperature (K). Eq. 4 gives a solubility value of $0.00018\ ppm$ at $550\ °C$ and $0.00026\ ppm$ at $600\ °C$, about 50 times lower than the estimate given by the law in Baus, Bogard et al. [20] (Eq. 3).

For $\mathbf{550}$ and $\mathbf{600\ °C}$, the solubility of metallic iron in liquid sodium is very low, compared to the dissolved iron content measured in our experiments (Table 3). Therefore, the presence of atomic iron in liquid sodium under our experimental conditions can be neglected. As mentioned in the introduction, iron cannot precipitate as solid $\boldsymbol{Na-Fe-O}$ oxides because a higher dissolved oxygen content would be required [7]. We did not observe solid oxides on the iron surface either (Fig. 2). The effect of dissolved oxygen can be explained by the formation of one or more $\boldsymbol{Na-Fe-O}$ complexes, soluble in liquid sodium, as proposed in the literature [8-12].

From the above estimates, we can also validate our experimental protocol. It is assumed that the mass loss of the samples corresponds precisely to the amount of iron that ends up in liquid sodium. However, removing a sample requires lowering the bath temperature to 120°C (Fig. 1). The iron complex could then dissociate, leading to re-precipitation of the iron on the crucible walls at $\mathbf{120\ °C}$. If the dissociation of the complex was rapid during these thermal cycles, no chemical equilibrium between iron and oxygenated sodium should occur because the concentration of the iron complex would be reduced to a low value for each decrease in temperature to $\mathbf{120\ °C}$. The results obtained show that a chemical equilibrium was reached in each test (Figs. 4 and 6). Iron crystallization, if it exists, occurs in negligible proportions. We can conclude that the concentration of the complex remains stable in the liquid sodium bath even at low temperatures. These results unequivocally demonstrate that our experimental approach, based on the variation of the sample mass, is well-suited to measuring the iron concentration in the liquid sodium at equilibrium under the applied operating conditions.

4.2 The form of dissolved oxygen in liquid sodium

We will see in section 4.3 that the most likely form of the complex in agreement with our measurements is $NaFeO_2$. This complex thus contains one mol of Fe and two mol of O. The amount of iron present in the liquid sodium as a complex was measured here (Section 4.1 and Table 3). A material balance can be used to deduce the amount of dissolved oxygen consumed by the formation of the complex: it represents 0.7%, 2.7%, 4.1%, 5.6% and 24.4% of the initial dissolved oxygen concentration for the T550-50, T550-100, T550-200, T550-400 and T600-200 tests, respectively. Based on these results, the consumption of dissolved oxygen in forming the complex is negligible in most cases.

This result is in good agreement with the observations of Thorley [12]. He conducted a corrosion test of pure iron at $650\ °C$ and $20-25\ ppm$ of dissolved oxygen in a circulating mild steel loop with $\Delta T = 25\ °C$. He measured an increase in the iron dissolution rate as a function of w_O^{Na}.

[2] Unpublished work

However, no significant change in dissolved oxygen content was noticed during the test. According to Thorley [12], two options can explain this surprising result: either a tiny amount of dissolved oxygen is consumed in formation of the $Na-Fe-O$ complex, or this complex is unstable over a slight temperature variation. This second hypothesis is not plausible given our results since a chemical equilibrium was reached during the tests performed with the CORRONa device. Our calculations also confirmed that the corrosion product consumes a very tiny amount of dissolved oxygen, in agreement with the first scenario suggested by Thorley [12]. A third hypothesis would be that Thorley measured both the dissolved oxygen and the oxygen in the complex. Indeed, in Thorley's experiments, the dissolved oxygen content was determined by direct sampling of the liquid sodium and a distillation technique was used to analyze these samples.

The next step of our work is to establish an equilibrium law for iron in liquid sodium. In order to take into account cases where the consumption of dissolved oxygen by the formation of the complex is not negligible (e.g. at $600\,°C$), the initial dissolved oxygen concentration will be divided into two contributions: the dissolved oxygen concentration and the oxygen in the $NaFeO_2$ complex (Eq. 14). However, there is an assumption that does not take into account the presence of the complex in the liquid phase: oxygen activity is calculated using the $Na-O$ binary liquid phase model. This assumption is indeed justified since sodium and oxygen are the main elements in the liquid phase.

4.3 Determination of an equilibrium law

This section aims to determine the evolution of the iron concentration in liquid sodium at equilibrium as a function of both temperature and initial dissolved oxygen content.

4.3.1 Determination of the complex activity coefficient

This study assumes that the iron corrosion by liquid sodium in the presence of dissolved oxygen is due to the formation of soluble complexes in liquid sodium. In this case, dissolved oxygen reacts upon contact with solid iron to form a soluble complex at the solid iron / liquid sodium interface, according to a heterogeneous chemical reaction (Eq. 5). Na_xFeO_n might be Na_4FeO_3, Na_2FeO_2 or $NaFeO_2$. It is assumed here that the possible complexes have the same stoichiometry as the mixed solid oxides of iron and sodium detected under different corrosion conditions.

$$Fe_{(s)} + n \cdot O_{(dissolved)} + x \cdot Na_{(liq)} \overset{\Delta G_r}{\Leftrightarrow} Na_xFeO_{n_{(dissolved)}} \quad (5)$$

with $Fe_{(s)}$: pure solid iron, $O_{(dissolved)}$: dissolved oxygen in liquid sodium, $Na_xFeO_{n_{(dissolved)}}$: dissolved complex in liquid sodium, $Na_{(liq)}$: pure liquid sodium, n and x: stoichiometric coefficients and ΔG_r: Gibbs free energy change for the chemical reaction. Three combinations are therefore possible to form these complexes:

- Na_4FeO_3: $x = 4$ and $n = 3$.
- $NaFeO_2$: $x = 1$ and $n = 2$.
- Na_2FeO_2: $x = 2$ and $n = 2$.

The iron dissolution and thus the formation of Na_xFeO_n stop when the chemical equilibrium described by Eq. 5 is reached (Sections 3.2 and 3.3). In this case, the activities of the species in solution are related by the equilibrium constant, K, which depends only on temperature:

$$K = \frac{a_{Na_xFeO_n}}{a_{Fe} \cdot {a_{Na}}^x \cdot {a_O}^n} \quad (6)$$

with $a_{Na_xFeO_n}$, a_O, a_{Fe} and a_{Na}: the activities of dissolved Na_xFeO_n, dissolved oxygen, iron and liquid sodium respectively. The chosen reference state is pure solid Na_xFeO_n, pure body-centered cubic solid iron, pure liquid sodium and O_2 gas at the standard pressure of 1 atm. The chemical reaction corresponding to the formation of solid Na_xFeO_n is given by Eq. 7:

$$Fe_{(s)} + \frac{n}{2} \cdot {O_2}_{(g)} + x \cdot Na_{(liq)} \overset{\Delta G^\circ_{f,Na_xFeO_{n(s)}}}{\Longleftrightarrow} Na_xFeO_{n_{(s)}} \quad (7)$$

with $\Delta G^\circ_{f,Na_xFeO_{n(s)}}$: the standard Gibbs free energy of the formation of solid Na_xFeO_n. Data for Na_2O, Na_2FeO_2, $NaFeO_2$ and Na_4FeO_3 are given in Table 4.

Solid oxides	$\Delta G^\circ_f\ (kJ/mol), T\ (K)$	References
Na_2O	$-426.765 + 0.1904 \cdot T$	HSC 5.1 [28]
Na_4FeO_3	$-1214.17 + 0.34269 \cdot T$	Shaiu et al. [7]
Na_2FeO_2	$-777 + 0.20795 \cdot T$	Shaiu et al. [7]
$NaFeO_2$	$-701.7 + 0.18945 \cdot T$	Shaiu et al. [7]

Table 4. Standard Gibbs free energies of the formation of solid Na_2O, Na_4FeO_3, Na_2FeO_2 and $NaFeO_2$.

Hence, the law of mass action for the reaction given by Eq. 5 can be expressed using Eq. 8:

$$\Delta G_r = \Delta G^\circ_{f,Na_xFeO_{n(s)}} + RT \cdot \ln\left(\frac{a_{Na_xFeO_n}}{a_{Fe} \cdot {a_O}^n \cdot {a_{Na}}^x}\right) \quad (8)$$

where $a_{Fe} = 1$ (pure solid iron). Since Na is the main element in liquid sodium, a_{Na} can be evaluated using Raoult's law. Thus, $a_{Na} = x_{Na}$, with x_{Na} being the molar fraction of sodium. In order to evaluate a_O, Rivollier et al. [13] used Eq. 9, valid if the activity of oxygen in liquid sodium follows Henry's law:

$$a_O = \frac{x_O^{Na}}{x_O^{Na,sat}} \cdot \exp\left(\frac{\Delta G_{diss}}{RT}\right) \quad (9)$$

with x_O^{Na} and $x_O^{Na,sat}$: the mole fractions of dissolved oxygen in liquid sodium and at saturation. This calculation established for a $Na - O$ binary liquid phase is assumed to be valid for the $Na - Fe - O$ liquid phase since sodium and oxygen are the main elements (Section 4.2). ΔG_{diss} is the Gibbs free energy change for the following chemical reaction:

$$\frac{1}{2} \cdot {O_2}_{(g)} \overset{\Delta G_{diss}}{\Longleftrightarrow} O^{Na,sat}_{dissolved} \quad (10)$$

where $O^{Na,sat}_{dissolved}$ is the dissolved oxygen in liquid sodium at saturation. According to Rivollier et al. [13], ΔG_{diss} can be estimated using Eq. 11:

$$\Delta G_{diss} = \Delta G^\circ_{f,{Na_2O}_{(s)}} - 2\ \cdot RT \cdot \ln\left(1 - x_O^{Na,sat}\right) \quad (11)$$

with $\Delta G^{\circ}_{f,Na_2O_{(s)}}$: the standard Gibbs free energy of the formation of solid Na_2O (Table 4). The solubility of oxygen in liquid sodium in the weight fraction, $w_O^{Na,sat}$ (ppm), can be evaluated using Noden's law [19]:

$$\log\left(w_O^{Na,sat}\right) = 6.2571 - \frac{2444.5}{T} \tag{12}$$

with T: the temperature (K). $w_O^{Na,sat} \ll 1$ and therefore $x_O^{Na,sat} \ll 1$ at 550 and 600 °C. Eq. 11 shows that $\Delta G_{diss} \approx \Delta G^{\circ}_{f,Na_2O_{(s)}}$.

At thermodynamic equilibrium, the Gibbs free energy change for the reaction given by Eq. 8, $\Delta G_r = 0$. Thus, using Eq. 8 and Eq. 9, $a_{Na_xFeO_n}$ can be expressed as follows:

$$a_{Na_xFeO_n} = {x_{Na}}^x \cdot \left(\frac{x_O^{Na}}{x_O^{Na,sat}}\right)^n \cdot \exp\left(\frac{n \cdot \Delta G^{\circ}_{f,Na_2O_{(s)}} - \Delta G^{\circ}_{f,Na_xFeO_{n(s)}}}{RT}\right) \tag{13}$$

In our experiments, the liquid sodium contains only traces of dissolved elements or complexes (mole fractions less than $5.7 \cdot 10^{-4}$ for dissolved oxygen and $3.7 \cdot 10^{-5}$ for complex). Therefore, $x_{Na} \approx 1$. With this latter assumption, Eq. 14 evaluates the mole fraction of oxygen in liquid sodium.

$$x_O^{Na} = x_O^{Na,init} - n \cdot x_{Na_xFeO_n}^{Na,eq} = M_{Na}\left(\frac{w_O^{Na,init}}{M_O} - n \cdot \frac{w_{Fe}^{Na,eq}}{M_{Fe}}\right) \tag{14}$$

where $x_O^{Na,init}$ is the mole fraction of dissolved oxygen initially present in liquid sodium, $x_{Na_xFeO_n}^{Na,eq}$ is the mole fraction of the complex in liquid sodium at equilibrium, M_{Na}, M_O and M_{Fe} are the molar masses of sodium ($22.990\ g/mol$), oxygen ($15.999\ g/mol$) and iron ($55.845\ g/mol$) respectively. The evaluation of $a_{Na_xFeO_n}$ at 550 and 600 °C is given in Table 5.

T (°C)	w_O^{Na} (ppm)	$a_{Na_4FeO_3}$	$a_{Na_2FeO_2}$	a_{NaFeO_2}
550	50	$9.2 \cdot 10^2$	9.76	$1.5 \cdot 10^{-3}$
	100	$6.7 \cdot 10^3$	37.5	$5.8 \cdot 10^{-3}$
	200	$5.1 \cdot 10^4$	147	$2.3 \cdot 10^{-2}$
	400	$3.7 \cdot 10^5$	565	$8.7 \cdot 10^{-2}$
600	200	$8.5 \cdot 10^3$	79.6	$2.3 \cdot 10^{-2}$

Table 5. Evaluation of $a_{Na_xFeO_n}$ at 550 and 600 °C, and at different dissolved oxygen contents.

Table 5 shows that $a_{Na_4FeO_3}$ and $a_{Na_2FeO_2}$ are greater than 1, which is not possible. These two stoichiometries can then be eliminated. $a_{NaFeO_2} < 1$ under the different experimental conditions. Therefore, the dissolved iron in liquid sodium is thought to be only in the form of the $NaFeO_2$ complex.

Fig. 7 shows the evolution of a_{NaFeO_2} as a function of $x_{NaFeO_2}^{Na,eq}$, at 550 °C. As a first approximation, the activity of the complex can be expressed using Henry's law:

$$a_{NaFeO_2} = \gamma^{\circ}_{NaFeO_2} \cdot x_{NaFeO_2}^{Na,eq} \tag{15}$$

with $\gamma^{\circ}_{NaFeO_2}$ the Henry's law constant. $\gamma^{\circ}_{NaFeO_2}$ is assumed to depend only on temperature. Hence, the evaluation of $\gamma^{\circ}_{NaFeO_2}$ at 550 and 600 °C gives 5234 ± 350 (average value) and 659 respectively. $\gamma^{\circ}_{NaFeO_2}$ can be expressed as a function of temperature as follows using these two values:

$$\log\left(\gamma^{\circ}_{NaFeO_2}\right) = -12.0 + \frac{12939}{T} \tag{16}$$

This law is based on two temperatures only. It must be refined with additional temperatures.

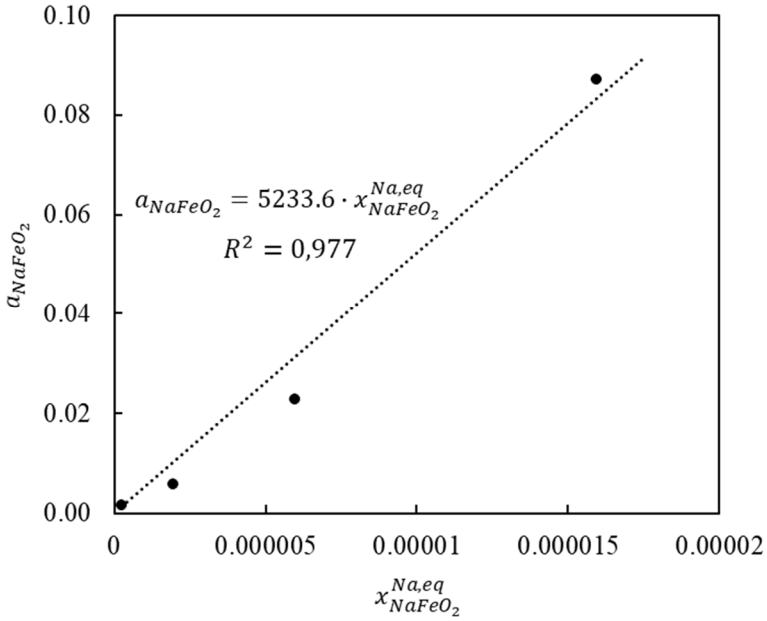

Fig. 7. Evolution of a_{NaFeO_2} as a function of $x^{Na,eq}_{NaFeO_2}$ at 550 °C.

4.3.2 Equilibrium law of iron in liquid sodium for $w_O^{Na} \geq 50\ ppm$

Eqs. 13, 14 and 15 will be used to develop an analytical law for the dissolved iron concentration in liquid sodium at equilibrium, as a function of dissolved oxygen concentration and temperature. The complex formed is $NaFeO_2$ and $x_{Na} \approx 1$ (section 4.3.1).

$$x^{Na,eq}_{NaFeO_2} = \frac{1}{\gamma^{\circ}_{NaFeO_2}} \cdot \left(\frac{x_O^{Na,init} - 2 \cdot x^{Na,eq}_{NaFeO_2}}{x_O^{Na,sat}} \right)^2 \cdot \exp\left(\frac{2 \cdot \Delta G^{\circ}_{f,Na_2O_{(s)}} - \Delta G^{\circ}_{f,NaFeO_{2(s)}}}{RT} \right) \tag{17}$$

For simplification, $2 \cdot \Delta G^{\circ}_{f,Na_2O_{(s)}} - \Delta G^{\circ}_{f,NaFeO_{2(s)}}$ is denoted ΔG°_f. Rearranging Eq. 17 yields a second-order equation, where $x^{Na,eq}_{NaFeO_2}$ is the unknown:

$$\left(x^{Na,eq}_{NaFeO_2}\right)^2 - \left(\frac{\gamma^{\circ}_{NaFeO_2} \cdot \left(x_O^{Na,sat}\right)^2}{4 \cdot \exp\left(\frac{\Delta G^{\circ}_f}{RT}\right)} + x_O^{Na,init} \right) \cdot x^{Na,eq}_{NaFeO_2} + \frac{\left(x_O^{Na,init}\right)^2}{4} = 0 \tag{18}$$

There are two possible solutions to this second-order equation. Only one of these solutions, given by Eq. 19, agrees with the experimental values of $x^{Na,eq}_{NaFeO_2}$, obtained during the five tests performed. The expression of $x^{Na,eq}_{NaFeO_2}$ is thus:

$$x_{NaFeO_2}^{Na,eq} = \frac{\alpha}{\beta} \cdot \left(1 - \sqrt{1 + \frac{\beta \cdot x_O^{Na,init}}{\alpha}}\right) + \frac{x_O^{Na,init}}{2} \tag{19}$$

with $\alpha = \gamma^{\circ}_{NaFeO_2} \cdot \left(x_O^{Na,sat}\right)^2$ and $\beta = 8 \cdot \exp\left(\frac{\Delta G_f^{\circ}}{RT}\right)$.

ΔG_f° and thus β can be evaluated as a function of temperature using the data from Table 4. α is calculated with Eqs. 12 and 16 as a function of temperature. Since the liquid sodium is almost pure, as a first approximation, we can write:

$$\begin{aligned} x_{NaFeO_2}^{Na,eq} &\approx \frac{M_{Na}}{M_{Fe}} \cdot w_{Fe}^{Na,eq} \\ x_O^{Na,init} &\approx \frac{M_{Na}}{M_O} \cdot w_O^{Na,init} \end{aligned} \tag{20}$$

Finally, $w_{Fe}^{Na,eq}$ can be calculated as a function of temperature and the initial oxygen mass fraction, $w_O^{Na,init}$. The condition that $x_{Na} \approx 1$, i.e. that the molar fractions of the elements or complexes in solution are negligible with respect to 1, is always satisfied. Thus, an equilibrium law for dissolved iron in liquid sodium is obtained by replacing the constants in Eq. 18 by their numerical values:

$$w_{Fe}^{Na,eq} = a \cdot 10^{\frac{8050}{T}} \cdot \exp\left(\frac{18262}{T}\right) \cdot \left(1 - \sqrt{1 + b \cdot 10^{-\frac{8050}{T}} \cdot \exp\left(\frac{-18262}{T}\right) \cdot w_O^{Na,init}}\right) + \mathrm{c} \cdot w_O^{Na,init} \tag{21}$$

with $w_{Fe}^{Na,eq}$ and $w_O^{Na,init}$ in ppm, $a = 2.070 \cdot 10^{-16}$, $b = 1.686 \cdot 10^{16}$, $c = 1.745$ and T: the temperature (K).

With the experimental conditions used here, $w_{Fe}^{Na,eq}$ follows a power law with an order very close to 2, as a function of $w_O^{Na,init}$ (Fig. 5). In Eq. 14, we considered the oxygen consumption involved in the complex. The measurements obtained for $x_{Na_xFeO_n}^{Na,eq}$ show that $x_O^{Na} \approx x_O^{Na,init}$ (Table 3). If this assumption is valid, the law of mass action leads to the following simplified equation and shows dependence on a power law of the order of 2:

$$\begin{aligned} x_{NaFeO_2}^{Na,eq} &= \frac{1}{\gamma^{\circ}_{NaFeO_2}} \cdot \left(\frac{x_O^{Na,init}}{x_O^{Na,sat}}\right)^2 \cdot \exp\left(\frac{\Delta G_f^{\circ}}{RT}\right) \\ w_{Fe}^{Na,eq} &= \frac{M_{Fe} M_{Na}}{{M_O}^2} \cdot \frac{\beta}{8 \cdot \alpha} \cdot \left(w_O^{Na,init}\right)^2 \\ w_{Fe}^{Na,eq} &= 7.374 \cdot 10^{15} \cdot 10^{-\frac{8050}{T}} \cdot \exp\left(\frac{-18262}{T}\right) \cdot \left(w_O^{Na,init}\right)^2 \end{aligned} \tag{22}$$

with $w_{Fe}^{Na,eq}$ and $w_O^{Na,init}$ in ppm and T: the temperature (K).

The law of mass action applied to our experimental results confirms that the stoichiometry of the complex cannot be Na_4FeO_3.

For the remainder of this study, we investigate the validity of the equilibrium law for the low dissolved oxygen contents (section 4.3.3) and compare the results obtained with experimental data from the literature (section 4.4).

4.3.3 Validity of the equilibrium law for low oxygen content

In the general case, iron can dissolve in liquid sodium in atomic or complex form. The iron concentration in liquid sodium at equilibrium is then equal to the sum of the two contributions:

$$w_{Fe}^{Na,eq} = w_{Fe\ in\ complex}^{Na,eq} + s_{Fe}^{Na} \tag{23}$$

with $w_{Fe\ in\ complex}^{Na,eq}$: the weight fraction of iron involved in $NaFeO_2$ complex in liquid sodium at equilibrium (ppm) and s_{Fe}^{Na}: the solubility of atomic iron in liquid sodium (ppm). In Eq. 21 established for $w_O^{Na,init} \geq 50\ ppm$, $w_{Fe}^{Na,eq} \approx w_{Fe\ in\ complex}^{Na,eq}$ since the liquid sodium is initially saturated in atomic iron (section 2.1).

The validity of our equilibrium law must be checked for low dissolved oxygen content ($w_O^{Na} < 50\ ppm$). It is to determine the dissolved oxygen content, from which the atomic iron solubility can be neglected with respect to the iron content in the $NaFeO_2$ complex. For this purpose, an arbitrary condition, given by Eq. 24, has been set:

$$w_{Fe\ in\ complex}^{Na,eq} > 10 \cdot s_{Fe}^{Na} \tag{24}$$

According to Baus, Bogard et al. [20], $w_{Fe\ in\ complex}^{Na,eq}$ must be greater than $0.1\ ppm$ at $550\ °C$ (Eq. 3). Application of our equilibrium law (Eq. 21) shows that $20\ ppm$ of dissolved oxygen is required to reach this value. On the other hand, $w_{Fe\ in\ complex}^{Na,eq}$ must be greater than $0.002\ ppm$, when applying Polley and Skyrme's law (Eq. 4). In this case, our equilibrium law shows that only $3\ ppm$ of dissolved oxygen is necessary to satisfy the condition given by Eq. 21.

The law of Baus, Bogard et al. is the most widely accepted in current work. Under normal operating conditions, liquid sodium has a dissolved oxygen concentration lower than or equal to $20\ ppm$ [1]. Therefore, it seems relevant to consider the two contributions of iron in atomic and complex form to establish a corrosion model.

4.4 Comparison with data in the literature

One of the main requirements for determining the corrosion mechanism of iron by liquid sodium is knowledge of the solubility of iron in liquid sodium. This thermodynamic data has been recognized as important for a long time. Solubility of iron in liquid sodium was measured from the early 1950s until the early 1980s. However, as shown in Fig. 8, the data obtained by different authors on the dissolved iron concentration in liquid sodium at equilibrium are widely scattered. All the experimental data in Fig. 8 appear to increase with temperature for the same chosen reference. In contrast, the effect of dissolved oxygen is more complex to interpret. For example, the equilibrium values obtained by Eichelberger and McKisson [23] and Rodgers et al. [24] at lower dissolved oxygen contents (2 and $20\ ppm$, respectively) are greater than those obtained by Stanaway and Thompson [25] at a higher dissolved oxygen content ($360\ ppm$). The scatter reported in Fig. 8 demonstrates the difficulty of obtaining reliable data. As discussed in Section 1,

the sampling and analysis methods applied by the authors must be considered when dealing with such scattered data.

The equilibrium law based on our experimental measurements (Eq. 21) overcomes these sampling and analysis issues since only the mass variation of the samples is measured. It allows us to understand the effect of dissolved oxygen by introducing the formation of a soluble complex in liquid sodium. This complex explains the increase in the solubility of iron in liquid sodium when the dissolved oxygen content increases. Indeed, in the absence of dissolved oxygen, $w_{Fe}^{Na,eq}$ is equal to s_{Fe}^{Na}, which results from the thermodynamic equilibrium between solid iron and liquid sodium. However, in the presence of dissolved oxygen, this equilibrium point is modified by the chemical interaction between dissolved oxygen and solid iron.

Our law (Eq. 21), called CORRONa law, is shown as a function of temperature for different dissolved oxygen contents in Fig. 8. The order of magnitude of the iron concentration in liquid sodium from the calculation agrees with the experimental results.

For $20\,ppm$ of dissolved oxygen, the CORRONa law provides a good reproduction of the experimental data of Singer et al. [21] and Stanaway and Thompson [25]. These data were obtained at low dissolved oxygen contents using a radiochemical counting technique. In contrast, the equilibrium values obtained by Rodgers et al. [24] at $20\,ppm$ appear to be ten times higher than the CORRONa law prediction. However, it should be noted that the authors did not observed any change in $w_{Fe}^{Na,eq}$, when the dissolved oxygen level was increased from 20 to $450\,ppm$. In addition, they did not mention any sodium purification steps before carrying out the tests. Thus, the fact that these data do not correspond to the predictions made by the CORRONa law could be due to the difficulties in controlling the sodium chemistry.

Thorley and Tyzack [26] reported a slight change in $w_{Fe}^{Na,eq}$ from 7 to $10\,ppm$, when the oxygen content increases from 10 to $100\,ppm$. This result is not in close agreement with the CORRONa law since our experimental data for $w_{Fe}^{Na,eq}$ follow a power law of order ≈ 2 as a function of the dissolved oxygen content (Fig. 5). Thus, a 10-fold increase in dissolved oxygen content results in a 100-fold increase in $w_{Fe}^{Na,eq}$.

The temperature dependence of the laws developed by Stanaway and Thompson [25] and by Epstein [27] at higher oxygen contents show a linear increase of $w_{Fe}^{Na,eq}$ with temperature, rather than an exponential increase as proposed by our analytical law. Our law is based on the law of mass action, a proven thermodynamic theory. However, only two temperatures (550 and $600\,°C$) were used to measure $w_{Fe}^{Na,eq}$ with the CORRONa device. In addition, only one measurement of $w_{Fe}^{Na,eq}$ at $600\,°C$ was performed. Additional measurements of $w_{Fe}^{Na,eq}$ must be performed at different temperatures to refine the values of the numerical coefficients present in the law.

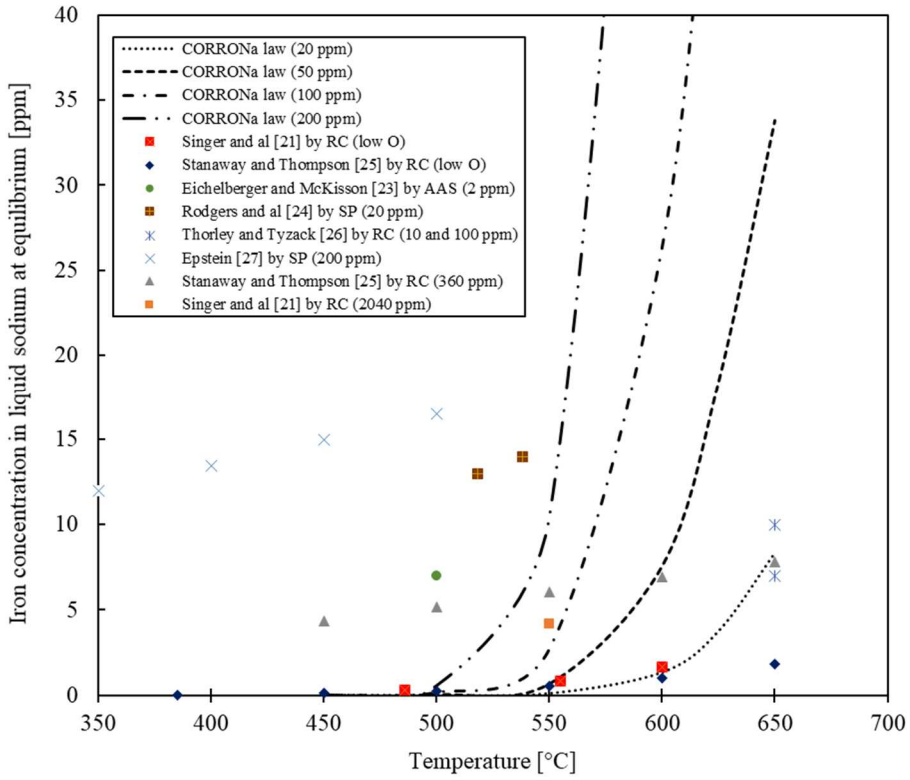

Fig. 8. Evolution of the dissolved iron concentration in liquid sodium at equilibrium as a function of temperature and at different dissolved oxygen contents. Comparison of the CORRONa law with the literature data reported by Awasthi and Borgstedt [2]. RC: radiochemical, SP: spectrometry and AAS: atomic absorption spectrometry.

4.5 Evaluation of the complex solubility

This last section aims to evaluate the iron concentration in liquid sodium at saturation, i.e. in equilibrium with the solid complex. The activity of the complex, with the reference state of liquid sodium saturated with the solid complex, can be expressed using Eq. 25:

$$a'_{NaFeO_2} = \frac{x_{NaFeO_2}^{Na,eq}}{x_{NaFeO_2}^{Na,sat}} \tag{25}$$

with $x_{NaFeO_2}^{Na,eq}$ and $x_{NaFeO_2}^{Na,sat}$: respectively the mole fractions of the complex in liquid sodium at equilibrium measured in this paper, and saturation in equilibrium with solid $NaFeO_2$.

a'_{NaFeO_2} can be expressed as a function of a_{NaFeO_2} the activity of the complex with the reference state of pure solid $NaFeO_2$ using Eq. 26:

$$RT \cdot \ln\left(a'_{NaFeO_2}\right) = RT \cdot \ln\left(a_{NaFeO_2}\right) - \Delta G_{diss,2} \tag{26}$$

with $\Delta G_{diss,2}$: the Gibbs free energy change for the following chemical reaction:

$$NaFeO_{2(s)} \overset{\Delta G_{diss,2}}{\Longleftrightarrow} NaFeO_2^{Na,sat}{}_{(dissolved)} \tag{27}$$

At saturation, $NaFeO_{2(s)}$ and $NaFeO_{2(dissolved)}$ are in equilibrium. Thus, $\Delta G_{diss,2} = 0$ and $a'_{NaFeO_2} = a_{NaFeO_2}$. Combining Eqs. 15, 20 and 25, it is found that:

$$x_{NaFeO_2}^{Na,sat} = \frac{1}{\gamma^{\circ}_{NaFeO_2}}$$
$$w_{Fe}^{Na,sat} = \frac{M_{Fe}}{M_{Na}} \cdot \frac{1}{\gamma^{\circ}_{NaFeO_2}} \quad (28)$$
$$log\left(w_{Fe}^{Na,sat}\right) = 18.4 - \frac{12939}{T}$$

with $w_{Fe}^{Na,sat}$: the iron solubility in liquid sodium saturated with solid $NaFeO_2$ expressed in ppm for the numerical application and T: the temperature (K). The evaluation of $w_{Fe}^{Na,sat}$ at 550 and 600 °C, gives respectively $480 \pm 30\ ppm$ (average value) and $3810 \pm 260\ ppm$.

5. Conclusion

Our work is part of research work aiming to guarantee the lifetime of 316L(N) steel in a sodium-cooled fast reactor. The objective is to determine the iron concentration in liquid sodium at equilibrium, $w_{Fe}^{Na,eq}$, as a function of temperature and dissolved oxygen content. A series of tests were carried out in the CORRONa device under isothermal conditions (550 °C or 600 °C) and at different dissolved oxygen contents (50, 100, 200 and 400 ppm) to develop an equilibrium law based on the sample mass variation. Compared to methods commonly used in the literature, the main advantage of our experimental approach is to avoid sodium sampling and analysis after solidification. The latter method leads to inhomogeneity and segregation, resulting in inaccurate equilibrium concentrations.

After exposure to liquid sodium, the surface of the samples was characterized using a scanning electron microscope. The characterization confirmed that, under our operating conditions, the corrosion mechanism of pure iron by liquid sodium is homogeneous dissolution. This allows us to validate the method of monitoring the corrosion kinetics from the mass loss.

During each test, the mass of dissolved iron increases as a function of time and reaches a plateau. The plateau is consistent with establishment of a chemical equilibrium in solution, meaning that the iron dissolution stops. The results showed that $w_{Fe}^{Na,eq}$, at 550 °C, follows a power law of order 2 as a function of the initial oxygen content. An additional test was performed at a higher temperature of 600 °C to study the effect of temperature on $w_{Fe}^{Na,eq}$. It appears that, for the same dissolved oxygen content, increasing the temperature by 50 °C leads to an increase in $w_{Fe}^{Na,eq}$ by a factor ~6.

In this study, it is found that the increase in $w_{Fe}^{Na,eq}$, in the presence of a high dissolved oxygen content, is directly related to the formation of a soluble complex in liquid sodium. Indeed, it is demonstrated that dissolved oxygen reacts with solid iron to form a soluble complex at the solid iron / liquid sodium interface. Based on the results obtained, the complex stoichiometry is thought to be $NaFeO_2$. The experimental results are then modelled using the law of mass action. An analytical law predicting the iron concentration in liquid sodium at equilibrium was developed for oxygen contents above 50 ppm as a function of temperature and dissolved oxygen content. The contribution of atomic iron is not considered in this equilibrium law. Indeed, the liquid sodium used in this study was initially saturated with atomic iron. The validity of this law for low oxygen contents has been discussed. It is quite possible to extrapolate this law to low dissolved oxygen contents, provided that the contribution of atomic iron is also taken into account.

This approach is a first step towards a model of iron corrosion by liquid sodium and thus improves our understanding of dissolution and deposition processes in liquid sodium systems.

Acknowledgements

The authors are extremely grateful to the CEA-Generation 4/Structural material project for the financial support received.

References

[1] H.U. Borgsted, C.K. Mathews, Applied Chemistry of the Alkali Metals, Plenum Press, New-York, 1987, pp. 183–184.

[2] S.P. Awasthi and H.U. Borgstedt, An Assessment of Solubility of Some Transition Metals (Fe, Ni, Mn and Cr) in Liquid Sodium, Journal of Nuclear Materials, Vol. 116, 1983, p.103-111.

[3] M. G. Barker and D. J. Wood, The Corrosion of Chromium, Iron, and Stainless Steel in Liquid Sodium, Journal of the Less-Common Metals, Vol. 35, 1974, p. 315-323.

[4] J. Zhang, T.F. Marcille, R. Kapernick, Theoretical Analysis of Corrosion by Liquid Sodium and Sodium-Potassium Alloys, Corrosion 64-7 , 2008, p. 563-573.

[5] C. Maury, J-B. Sirven, M. Tabarant, D. L'Hermite, J-L. Courouau, C. Gallou, N. Caron, G. Moutiers and V. Cabuil, Analysis of Liquid Sodium Purity by Laser-Induced Breakdown Spectroscopy. Modeling and Correction of Signal Fluctuation Prior to Quantitation of Trace Elements, Spectrochimica Acta Part B: Atomic Spectroscopy, Vol. 82, 2013, p. 28-35.

[6] E. Yoshida, T. Furukawa, Corrosion Issues in Sodium-Cooled Fast Reactor (SRF) Systems, in: D. Féron (Ed), Nuclear Corrosion Science and Engineering, Woodhead Publishing Limited – Cambridge, Philadelphia, 2012, p. 773-806.

[7] B.J. Shaiu, P.C.S. Wu, P. Chiotti, Thermodynamic Properties of the Double Oxide of Na2O with the Oxides of Cr, Ni and Fe, Journal of Nuclear Materials, Vol. 67, 1977, p. 13-23.

[8] J.R. Weeks, H.S. Isaacs, Corrosion and deposition of steels and nickel-base alloys in liquid sodium, Advances in Corrosion Science and Technology, Vol. 3, Plenum Press, New York, London, 1973, p. 1-66.

[9] B.H. Kolster, Mechanism of Fe and Cr Transport by Liquid Sodium in a Non-Isothermal Loop System, Journal of Nuclear Materials, Vol. 55, 1975, p. 155-168.

[10] G. W. Horsley, Corrosion of Iron by Oxygen-Contaminated Sodium, Journal of the Iron and Steel Institute, Vol. 282, 1956, p. 43. Originally U.K. Report A.E.R.E . M/R 1441, 1954.

[11] J. D. Mottley, Sodium Mass Transfer: VIII Corrosion of Stainless Steel in Isothermal Regions of a Flowing Sodium System, USAEC Report GEAP-4313, General Electric Company, Vallecitos Atomic Laboratory, 1964.

[12] A. W. Thorley, The Corrosion of Iron in Sodium and the Influence of Alloying Elements on its Mass Transfer Behavior. Materials Behavior and Physical Chemistry in Liquid Metal Systems, Karlsruhe, 1981, Plenum. Press. p. 19.

[13] M. Rivollier, J.-L. Courouau, M. Tabarant, C. Blanc, M.-L. Giorgi, Oxidation of 316L (N) Stainless Steel in Liquid Sodium at 650 °C, Journal of Nuclear Materials, Vol. 500, 2018, p. 337–348.

[14] M. Rivollier, J. L. Courouau, M. L. Giorgi, Further insights into the mechanisms involved in the corrosion of 316L(N) austenitic steel in oxygenated liquid sodium at 550 °C, Corrosion Science, Vol. 165, 2020, 108399.

[15] J.L. Courouau, F. Balbaud-Célérier, V. Lorentz, T. Dufrenoy, Corrosion by Liquid Sodium of Materials for Sodium Fast Reactors: The CORRONa Testing Device, The Proceedings of the International Congress on Advances in Nuclear Power Plants (ICAPP' 11), Paper 11152, Nice, France 2-5 May 2011.

[16] F. Rouillard, J.-L. Courouau, B. Duprey, S. Mathieu, M. Vilasi, Y. Bouizi, G. Boissonnet, F. Pedraza, I. Proriol-Serre, Evaluation of The Compatibility of Aluminide Coatings in High-Temperature Sodium for Fast Reactor Application, Oxidation of metals, Vol. 88, 2017, p. 221-233.

[17] B.H. Kolster, L. Bos, Sodium Corrosion in a Total Molybdenum Loop System: Construction, Experience and Results, in: Liquid Metal Engineering and Technology, The British Nuclear Energy Society, London, 1984, p. 235-242.

[18] Eberhart, J. G., F. A. Cafasso, H. M. Feder and W. Kremsner, The Grain Boundary Grooving of Iron in Liquid Sodium, In Corrosion by Liquid Metals: Proceedings of the Sessions on Corrosion by Liquid Metals of the 1969 Fall Meeting of the Metallurgical Society of AIME, October 13–16, 1969, Philadelphia, Pennsylvania. Edited by J. E. Draley and J. R. Weeks, 461-67. Boston, MA: Springer US, 1970.

[19] J.D. Noden, A general Equation for the Solubility of Oxygen in Liquid Sodium, Journal of the British Nuclear Energy Society, Vol. 12 (1), 1937, p. 57-62 and 329-331.

[20] R. A. Baus, A. D. Bogard, J. A. Grand, L. B. Lockhart, R. R. Miller and D. D. Williams, The Solubility of Structural Materials in Sodium, Proceedings of the First United Nations International Conference on Peaceful Uses of Atomic Energy, Geneva, Vol. 9, 1955, p. 356.

[21] R.M. Singer, A.H. Fleitman, J.R. Weeks et H.S. Isaacs, Measurements of the Solubility of Iron and Chromium in Sodium, in Corrosion by Liquid Metals, Proceedings of the sessions on corrosion by liquid Metals of the 1969 fall meeting of the metallurgical society of AIME, October 13-16, 1969, Philadelphia, Pennsylvania, New York - London : Plenum Press 1970, p .561-576.

[22] M.V. Polley, G. Skyrme, An Analysis of the Corrosion of Pure Iron in Sodium Loop Systems, Journal of Nuclear Materials, Vol. 66, 1977, p. 221-235.

[23] R.L. Eichelberger and R.L. McKisson, Studies of the Solubility of Iron in Sodium, Atomics International, A Division of North American Aviation, AI-AEC-12834, 1969.

[24] S.J. Rodgers. J.W. Mausteller and E.F. Batutis, Iron and Nickel Concentration in Sodium, Mine Safety Appliance Co. Rep. MSA-TR-27, 1954.

[25] W.P. Stanaway and R. Thompson, Solubility of metals, iron and manganese in sodium, Second International Conference on Liquid Metal Technology in Energy, Richland, Washington, 1980, p. 18-54.

[26] A. W. Thorley and C. Tyzack, Corrosion Behavior of Steels and Nickel Alloys in High Temperature Sodium, Alkali Metal Coolants IAEA, 1967 Vienna, p. 97-118.

[27] L. F. Epstein, Preliminary studies of the solubility of iron in liquid sodium, Science 112, 1950, p. 426.

[28] A. Roine, Outokumpu HSC Chemistry for Windows, Version 5.1, 2002.